Dalton Transactions

Versatility of Cyclooctatetraenyl Ligands in Rare Earth Metal Complexes of the [M2(COT)3(THF)2] (M = Y and La) Type

Journal:	*Dalton Transactions*
Manuscript ID	DT-ART-02-2019-000868.R1
Article Type:	Paper
Date Submitted by the Author:	27-Mar-2019
Complete List of Authors:	Greenough, Joshua; University at Albany State University of New York, Chemistry Zhou, Zheng; University at Albany State University of New York, Chemistry Wei, Zheng; University at Albany, SUNY, Chemistry Petrukhina, Marina; University at Albany State University of New York, Chemistry

Versatility of Cyclooctatetraenyl Ligands in Rare Earth Metal Complexes of the $[M_2(COT)_3(THF)_2]$ (M = Y and La) Type

Joshua Greenough, Zheng Zhou, Zheng Wei and Marina A. Petrukhina*

Department of Chemistry, University at Albany, State University of New York, Albany, NY 12222, USA

E-mail: mpetrukhina@albany.edu

Two new organometallic cyclooctatetraenyl complexes of the type $[M_2(COT)_3(THF)_2]$ (M = Y and La) have been prepared, using optimized synthetic procedures, and fully characterized by X-ray diffraction analysis, IR and ^{1}H NMR spectroscopies. The structures can be represented as formed by the double-decker $[M(COT)_2]^-$ anion with an asymmetrically bound cationic $[M(COT)(THF)_2]^+$ unit. The COT rings in the anionic sandwich are not equidistant from the metal with the M–$COT_{centroid}$ distances measuring at 1.991(5) Å and 2.074(5) Å for $[Y(COT)_2]^-$ *vs*. 2.045(4) Å and 2.154(5) Å for $[La(COT)_2]^-$. The sandwich fragments are η^2-coordinated to the second metal center with the average M–C distances of 2.837(4) Å and 2.879(5) Å for yttrium and lanthanum complexes, respectively. The M–$COT_{centroid}$ distances in the cationic unit are 1.962(4) Å for the former and 2.009(2) Å for the latter.

Introduction

Organometallic complexes of lanthanides (Lns) have sustained several decades of popularity, largely due to their utility in the fields of homogeneous catalysis[1] and materials science.[2] Within the broad family of organolanthanide complexes, the cyclooctatetraene dianion (COT) ligand is second most prominent, surpassed only by cyclopentadiene (Cp).[3] Contrary to COT's ubiquity, a limited structural variety of homoleptic complexes containing COT as the sole type of ligand have been crystallographically characterized. The first, and simplest, homoligated organolanthanide complexes reported were assigned *via* elemental analysis and EPR measurements to the Ln(COT) formulation (Ln = Eu, Yb), in which the metal center has a 2+ charge and is believed to be η^8-coordinated to COT.[4] From this prototypical "half-sandwich" type structure (**A**; Scheme 1), researchers gradually extended this basic building unit to include more layers. This progression lead to the discovery and X-ray structural characterization of cerocene, $Ce(COT)_2$.[5] This compound featured a single metal center, symmetrically sandwiched between two COT ligands bound in an η^8-fashion (**B**; Scheme 1). To accommodate the collective 4– charge from the COT ligands, Ce exhibits a 4+ oxidation state. A more common variation of this structure contains a sandwiched Ln^{3+} ion and is ballanced with a solvent-separated cation (**C**; Scheme 1).[6] Interestingly, some analogues of **C** have been known to dimerize, thus forming a linear tetranuclear structure (**D**; Scheme 1).[7]

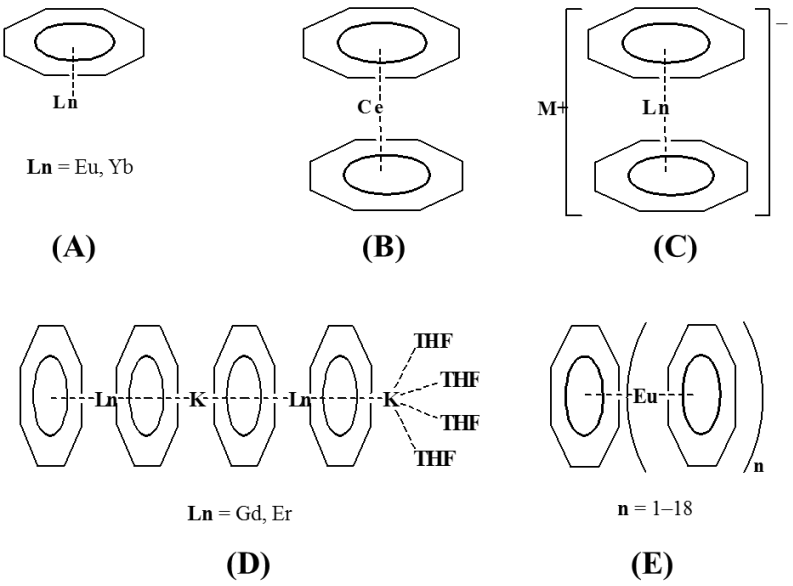

Scheme 1. Structural variety of homoligated organolanthanide COT complexes.

Given the limited number of Ln oxidation states, unwavering 2– charge associated with COT dianion, and difficulty in combining different lanthanides, preparation of more complex structural types has been elusive. Nakajima's group made a stride toward the development of higher structural complexity with the report on the $Eu_n(COT)_m$ nanowires (**E**; Scheme 1).[8] Impressively, the report claimed that these organometallic nanowires could be grown up to 18 layers long. Although these findings were supported by photoelectron and photoionization spectroscopies, it should be noted that no X-ray diffraction structural data were available. The additional type of the Ln(COT)-based structures reported in the literature is consistent with the formula $[M_2(COT)_3(THF)_2]$ (**F**; Scheme 2).

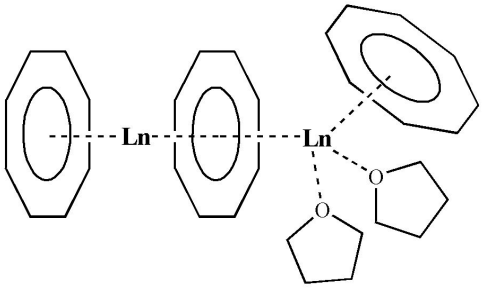

(F)

Scheme 2. Structure of a $[Ln_2(COT)_3(THF)_2]$ complex.

Similar to **C**, this structure has the charged $[Ln(COT)_2]^-$ fragment; however, it is balanced with an aditional $[Ln(COT)(THF)_2]^+$ unit (Scheme 3), instead of a Group 1 cation.

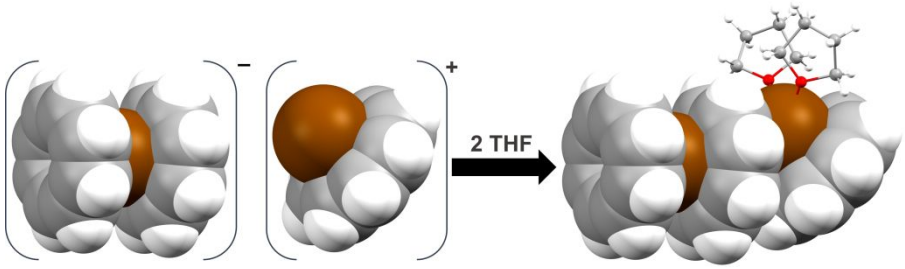

Scheme 3. Schematic formation of $[Ln_2(COT)_3(THF)_2]$ complex from two charged units.

This dimetal structural type was first discovered in the late 1970s by DeKock *et al.*, who reported the crystal structure of the Nd complex, $[Nd_2(COT)_3(THF)_2]$, and claimed to have also synthesized the La, Ce, and Er analogues.[9] To date, the above neodiumium(III) complex remained the only member of this family to be crystallographically characterized. Herein, we report, for the first time in nearly 40 years, two additional analogues of the formula $[M_2(COT)_3(THF)_2]$ with M = Y and La. Both complexes have been structurally characterized using single crystal X-ray diffraction analysis and spectroscopic methods.

Results and Discussion

The original synthesis of $[Ln_2(COT)_3(THF)_2]$ compounds, as detailed by DeKock and co-workers, required cocondensation of a given lanthanide metal with a large excess of COT (9–18 eq.) at very low temperature (–196 °C) and pressure (4×10^{-4} mmHg), for 30–60 minutes.[9] The product purification and crystal growth were accomplished via Soxhlet-extraction. The above synthetic technique required a special reaction apparatus, similar to the one developed by Streitwiser and co-workers to prepare uranocene, $U(COT)_2$.[10] We found that this type of products could be synthesized under much less extreme reaction conditions, without a huge excess of COT, and in far greater yield (~70% *vs.* 20%). Our optimized synthesis is based on the addition of 1.5 eq. of $K_2(COT)$ to a stirring solution of MI_3 (M = Y and La) in THF at room temperature (Scheme 4). The reaction is allowed to proceed to completion over 24 h. After that, the light-yellow mixture is filtered and the resulting yellow filtrate is sealed in an L-shaped ampule.

$$2MI_3 + 3K_2(COT) \xrightarrow[24\ h,\ r.t.]{THF} [M_2(COT)_3(THF)_2] + 6KI$$

Scheme 4. Preparation of $[M_2(COT)_3(THF)_2]$, M = Y (**1**) and La (**2**).

For crystal growth, the product-containing segment of the ampule was placed above a 140 °C sand-bath to facilitate slow solvent evaporation. After approximately 7–10 days, nearly all solvent had evaporated, thus affording yellow plate-shaped crystals along the bottom of the ampule in a very good yield (70–75%). Infrared spectra of both complexes were found to be nearly identical to one another and closely resemble the spectra collected by DeKock.[9] Additional characterization via ^{1}H NMR spectroscopy was conducted on **1** and **2**, representing

the first ^{1}H NMR study of the $[M_2(COT)_3(THF)_2]$ family (Figures S3-S6), as previous attempts to observe the proton magnetic resonance spectra have failed.[9] The room temperature data reflect on the fluxional behaviour of the systems, but a 2:1 integration of the two COT signals at 5.88 ppm and 6.28 ppm has been clearly observed at low (–80 °C) temperature (Figure 1).

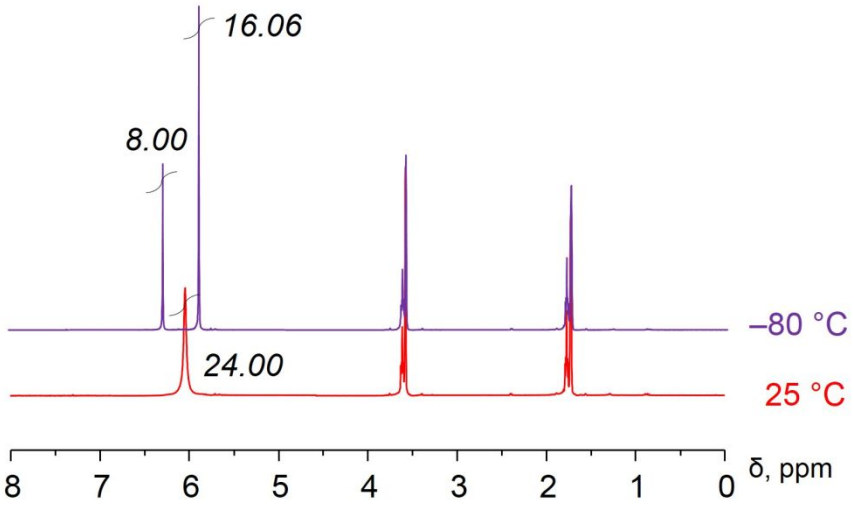

Figure 1. ^{1}H NMR spectra of **2** in THF-d_8 at 25 °C and –80 °C, with COT peaks integrated.

The X-ray diffraction studies confirmed the composition of the two products to be $[M_2(COT)_3(THF)_2]$ (M = Y, **1**) and (M = La, **2**) (Figure 2). Their molecular structures can be described as consisting of two charged building units (Scheme 3). The anionic part is formed by a M^{3+} ion sandwiched between two η^8-coordinated COT ligands. Then, one of the COT rings of the sandwich coordinates (η^2) to a second metal center, whose coordination environment is completed by a third η^8-bound COT ring and two THF solvent molecules.

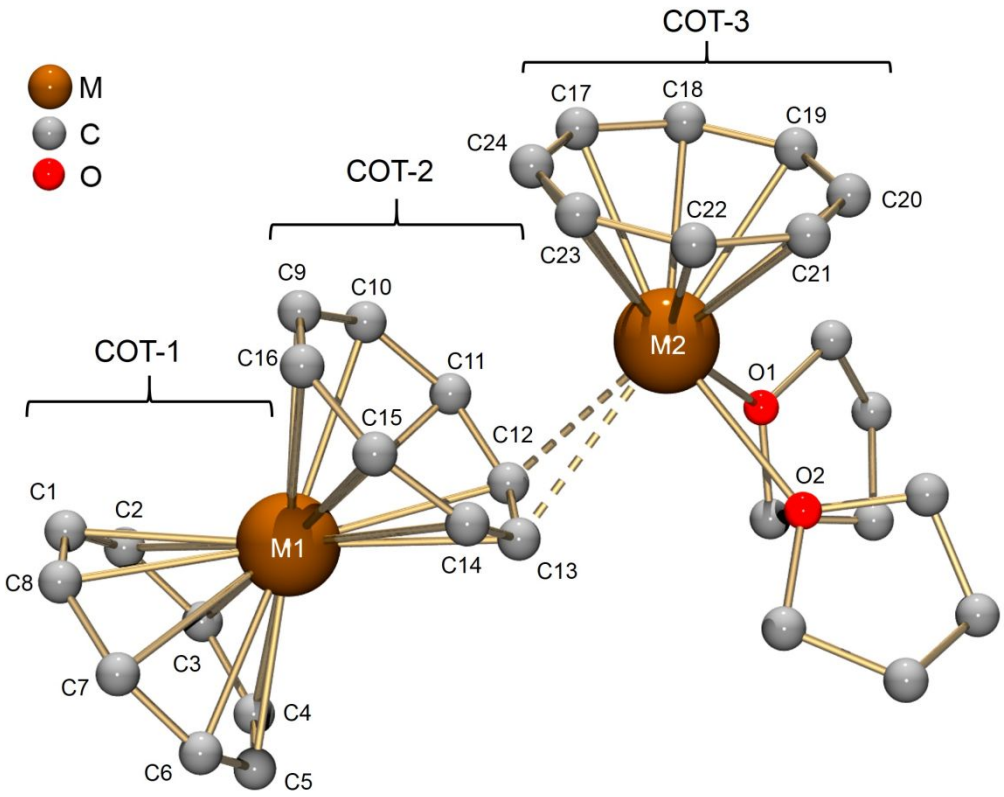

Figure 2. Ball-and-stick model of $[M_2(COT)_3(THF)_2]$ (hydrogen atoms are omitted for clarity).

In **1**, the average Y1–C_{COT1} and Y1–C_{COT2} bond length distances are 2.701(5) Å and 2.769(2) Å, respectively. The M–$COT_{centroid}$ distances measuring at 1.991(5) Å and 2.074(5) Å for $[Y(COT)_2]^-$ also show that the two COT rings in the anionic sandwich are not equidistant from the metal center. The two Y2–C_{COT2} bonds between the sandwich and the cationic $[Y(COT)(THF)_2]^+$ unit are measured at 2.899(5) and 2.775(5) Å. Lastly, the Y2–C_{COT3} bond length distances range from 2.666(4) to 2.720(4) Å. Comparison of the η^8-coordinated COT ligands revealed that the average Y–C bond length distances are the longest between COT1 and Y1 and are the shortest between Y2 and COT3 ($\Delta_{avg.}$ = 0.276(5) Å).

In **2**, the average La1–C_{COT1} and La1–C_{COT2} bond length distances are 2.745(4) Å and 2.850(2) Å, respectively. Again, the M–$COT_{centroid}$ distances of 2.045(4) Å and 2.154(5) Å show

that the two COT rings are not equidistant from a metal center in $[La(COT)_2]^-$. This sandwich fragment is η^2-coordinated to La2 with the bond length distances of 2.897(5) Å and 2.860(5) Å. The average La2–C_{COT3} bond length distance was determined to be 2.731(2) Å. Aside from the η^2-coordinated carbon atoms, average La–C_{COT} bond length distances were found to be the greatest between La2 and COT2 and the shortest between La2 and COT3 ($\Delta_{avg.}$ = 0.148(5) Å). All La–COT distances fall within the range of analogous distances found in the literature.[6k,6l]

Table 1. Selected bond length distances in $[Y_2(COT)_3(THF)_2]$ (**1**), $[La_2(COT)_3(THF)_2]$ (**2**) and $[Nd_2(COT)_3(THF)_2]$ (in Å).

	Y (**1**)	La (**2**)	Nd*
M1–$C_{COT1, avg}$	2.701(5)	2.745(4)	2.68(1)
M1–$C_{COT2, avg.}$	2.769(5)	2.850(5)	2.79(1)
M2–$C_{COT2, avg.}$	2.837(5)	2.879(5)	2.79(2)
M2–$C_{COT3, avg.}$	2.686(4)	2.731(2)	2.68(1)
M2–$O_{THF, avg.}$	2.558(3)	2.601(1)	2.58(2)
M^{3+} radius[11]	0.930	1.03	0.983
X-ray experiment temp. (K)	100(2)	100(2)	294

*X-ray diffraction experiment of the Nd complex was conducted at room temperature only.[9]

The M–C bond length distances range over 2.656(5)–2.899(5) Å and 2.703(2)–2.897(5) Å in **1** and **2**, respectively (Table S3). The longest bond in each structure is between M2 and COT3, presumably to mitigate unfavourable steric interaction between the tilted COT rings. Analysis of COT planarity showed that the three rings of each structure have relatively little deviation from an ideal plane, as expected due to their aromatic nature (Table 2).

Table 2. Estimation of planarity for COT rings in **1** and **2**.

	Root Mean Square Deviation (RMSD) of fitted atoms	
	(**1**)	(**2**)
COT1	0.0312	0.0060
COT2	0.0304	0.0465
COT3	0.0082	0.0190

For **1** and **2**, the $COT1_{centroid}$–M1–$COT2_{centroid}$ angles are 174.11° and 172.91°, respectively. This deviation from linearity can be attributed to COT2 demonstrating a slight bend away from COT3. In contrast to the nearly parallel orientation of COT1 and COT2, the planes of COT2 and COT3 were found to intersect at angles of 35.96° and 38.48° in **1** and **2**, respectively. As shown in Figure 3, the tilting of COT3 with respect to the $[M(COT)_2]^-$ unit would appear to compensate for the steric repulsion generated by the coordinated THF molecules.

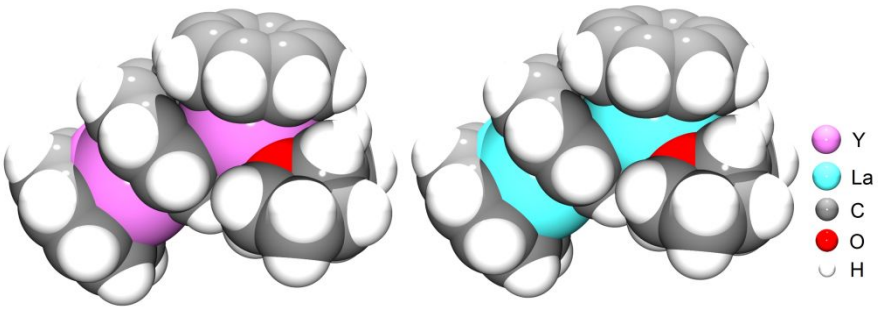

Figure 3. Space-filling depiction of **1** (left) and **2** (right).

In addition to M–C_{COT} distances, the M–O_{THF} bond length distances in **1** and **2** were measured and compared to relevant literature values. In **1**, THF molecules coordinate to Y2 at bond length distances of 2.562(3) Å and 2.553(3) Å. A survey of several structures, containing Y–O_{THF} bonds, revealed that those in **1** (Y–O_{THF} average, 2.558 Å) are longer than an average literature value of 2.393 Å.[12] In contrast, the average La–O_{THF} bond length distance of 2.601(1) Å in **2** is close to those found in literature.[6k,13]

Compounds **1** and **2** add two new crystallographically verified members to the family of $[Ln_2(COT)_3(THF)_2]$ complexes, the other known member being the Nd analogue. It should be noted here that the X-ray diffraction experiment of the neodymium complex was performed at room temperature[9] and, therefore, its direct structural comparison with **1** and **2** may be less accurate. The major bond distances of these three compounds can be found in Table 1. Expectedly, all main geometric parameters were found to be proportional to M^{3+} radius,[11] with the exception of the M1–$C_{COT1,\ avg}$ distance, which is longer in the Y complex compared to the Nd analogue. On average, the lanthanum complex exhibits the longest bond length distances, while the yttrium complex has the shortest corresponding bong length values.

A comparison of solid state packing of **1** and **2** revealed their close similarity. As shown in Figure 4, individual $[M_2(COT)_3(THF)_2]$ molecules link to one another *via* weak intrermolecular C–H···π interactions resulting in an extended 2D network. These intermolecular interactions range over 2.441(5)–2.780(5) Å and 2.453(5)–2.796(5) Å in **1** and **2**, respectively (Table S4). Although the ranges of C–H···π interactions are largely consistent, **1**, on average, exhibits slightly stronger C–H···π interactions than **2** (2.604(5) *vs.* 2.634(5) Å). No significant interactions between the neighboring 2D layers were detected.

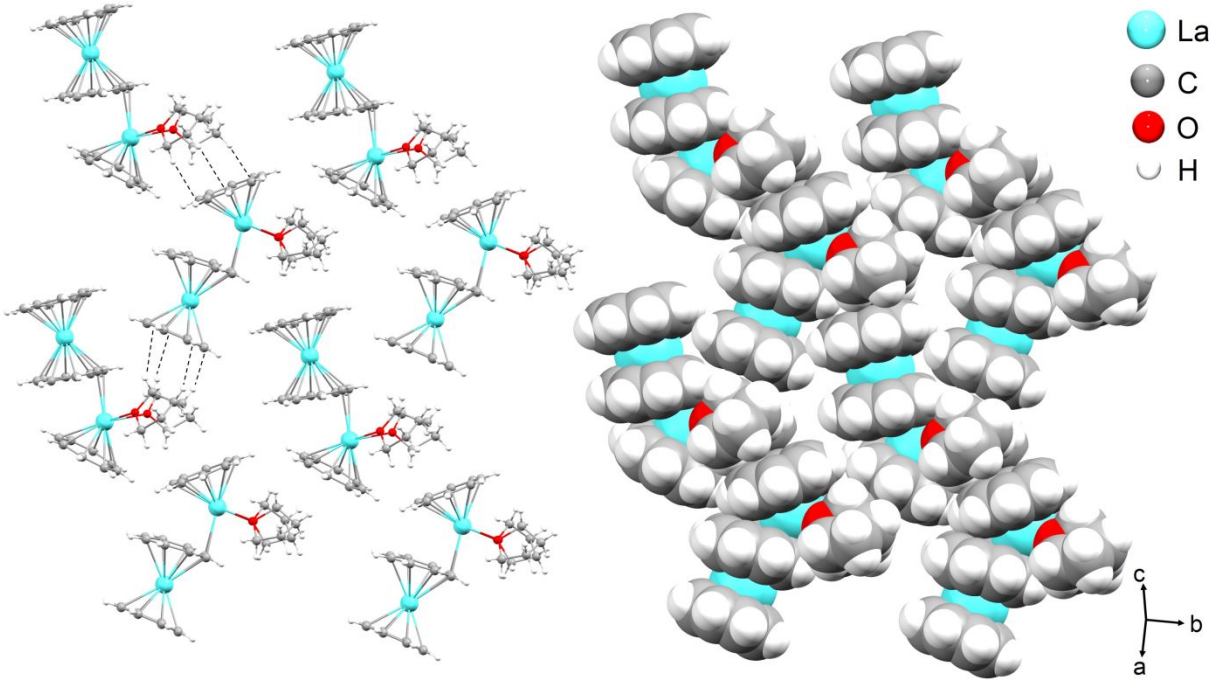

Figure 4. 2D layer in **2**, ball and stick model (left), space filling model (right).

In summary, an optimized, economical and easy-to-use procedure that does not rely on metal-atom evaporation approach has been developed for the synthesis of the $[M_2(COT)_3(THF)_2]$ complexes. Two new complexes of this stoichiometry with M = Y and La have been prepared in good yield as bulk crystalline materials and crystallographically characterized for the first time. A direct structural comparison of the yttrium and lanthanum complexes with the only known neodymium analogue clearly showed the dependance of major geometric parameters on the metal ion size. Notably, the isolation of asymmetric $[M_2(COT)_3(THF)_2]$ complexes with rare earth metals, M = Y and La, allowed their first ^{1}H NMR spectrocopic invesitigation, as previous attempts were not successful. This work adds new synthetic and structural advancements to the COT-based organometallic chemistry and provides a good platform for future development of polynuclear organolanthanide complexes with interesting magnetic properties.

Experimental Part

Materials and methods

The preparation and all manipulations were carried out using break-and-seal as well as Schlenk and glove-box techniques[14] under an atmosphere of argon. Tetrahydrofuran (THF) was purchased from Sigma Aldrich and dried over Na/benzophenone and distilled prior to use. Potassium and cyclooctatetraene were purchased from Sigma Aldrich. YI_3 and LaI_3 were purchased from Alfa Aesar. K_2COT was prepared according to literature[15] and stored in glove box. The attenuated total reflection (ATR) spectra were recorded on a PerkinElmer Spectrum 100 FT-IR spectrometer. The ^1H NMR spectra of **2** were measured on a Bruker AC-400 spectrometer at 400 MHz; the ^1H NMR spectra of **1** were measured on a Bruker Ascend-500 spectrometer at 500 MHz. The ^{13}C NMR spectrum of **2** was measured on a Bruker Ascend-500 spectrometer at 125 MHz. All spectra were referenced to the resonances of the corresponding solvent used.

Preparation of $Y_2(COT)_3(THF)_2$ (1). YI_3 (0.037 g, 0.079 mmol) was stirred in 8 mL of THF for 24 h until the solid was fully dissolved. Slow addition of K_2COT (0.022 g, 0.118 mmol, 1.5 eq.) in 3 mL THF to a violently stirred YI_3 solution produced a cloudy yellow solution in 35 min. This mixture was stirred for 24 h at room temperature to complete the reaction. All volatiles were then removed under vacuum and replaced with 7 mL of THF. The crude mixture was then allowed to stir for an additional 24 h before being passed through a fine frit-filter. The light yellow filtrate was sealed in an L-shaped ampule. The ampule was then placed 3 inches above a 140 °C sand-bath. After several days all solvent had evaporated leaving behind a light-yellow micro-crystalline product. Fresh THF (6 mL) was then used to rinse the solid. The resulting light

yellow solution was then transferred to a new L-shaped ampule, which was subjected to the same crystallization method as detailed above. After 10 days, almost all solvent had evaporated, leaving large yellow, plate-shaped crystals. Yield: 0.018 g, 72%. IR: 1014, 896, 864, 835, 784, 742, 707 and 688 cm^{-1}. ^1H NMR (500 MHz, THF-d_8, –80 °C, ppm): δ, 1.79 (m, 8H, C_4H_8O), 3.62 (m, 8H, C_4H_8O), 5.81 (s, 16H, $C_8H_8^{2-}$), 6.28 (s, 8H, $C_8H_8^{2-}$). ^1H NMR (500 MHz, THF-d_8, 25 °C, ppm): δ, 1.78 (m, 8H, C_4H_8O), 3.62 (m, 8H, C_4H_8O), 5.92 (s, 24H, $C_8H_8^{2-}$).

Preparation of $La_2(COT)_3(THF)_2$ (2). LaI_3 (0.035 g, 0.066 mmol) was stirred in 8 mL of THF for 1 h until all solids were fully dissolved. Slow addition of K_2COT (0.082 g, 0.102 mmol, 1.5 eq.) in 3 mL THF to a vigorously stirred LaI_3 solution produced a cloudy yellow solution in 35 min. This solution was stirred for an additional 24 h at room temperature to complete the reaction. The mixture was then concentrated to ~ 5 mL, before being passed through a fine filter into an L-shaped ampule. The ampule containing a light yellow filtrate was sealed under reduced pressure and placed 3 inches above a 140 °C sand-bath. After several days all solvent had evaporated, yielding small light-yellow crystals. Fresh THF (6 mL) was then used to rinse the solid. The resulting light-yellow solution was transferred to a new L-shaped ampule, which was then subjected to the same crystallization method as detailed above. After 10 days, almost all solvent had evaporated, leaving large yellow, plate-shaped crystals. Yield: 0.018 g, 74%. IR: 1015, 892, 862, 833, 780, 739, 711 and 688 cm^{-1}. ^1H NMR (400 MHz, THF-d_8, –80 °C, ppm): δ, 1.79 (m, 8H, C_4H_8O), 3.62 (m, 8H, C_4H_8O), 5.88 (s, 16H, $C_8H_8^{2-}$), 6.28 (s, 8H, $C_8H_8^{2-}$). ^1H NMR (400 MHz, THF-d_8, 25 °C, ppm): δ, 1.79 (m, 8H, C_4H_8O), 3.62 (m, 8H, C_4H_8O), 6.05 (s, 24H, $C_8H_8^{2-}$).

Crystal structure determination and refinement of 1 and 2

Data collection was performed on a Bruker D8 VENTURE X-ray diffractometer with a PHOTON 100 CMOS shutterless mode detector equipped with a Mo-target X-ray tube (λ = 0.71073 Å) at T = 100(2) K. Data reduction and integration were performed with the Bruker software package SAINT (version 8.38A).[16] Data were corrected for absorption effects using the empirical methods as implemented in SADABS (version 2016/2).[17] The structures were solved by SHELXT (version 2018/2)[18] and refined by full-matrix least-squares procedures using the Bruker SHELXTL (version 2018/3)[19] software package. All non-hydrogen atoms were refined anisotropically. All H atoms were included at calculated positions and refined as riders with U_{iso}(H) = 1.2 U_{eq}(C). In order to evaluate the planarity of COT rings, the least-squares plane is calculated through eight carbon atoms of each COT ring by applying an MPLA command during refinement. Further crystal and data collection details are listed in Table S1. See Supporting Information for ORTEP drawings and more structural details. CCDC are 1899492 and 1899493 for **1** and **2**, respectively.

Acknowledgments

Acknowledgment is made to the Donors of the American Chemical Society Petroleum Research Fund for support of this work through 54967ND3 grant. Partial support from the National Science Foundation, CHE-1608628, is also acknowledged.

References

1 (*a*) M. N. Bochkarev, *Chem. Rev.*, 2002, **102**, 2089–2117; (*b*) F. T. Edelmann, *Coord. Chem. Rev.*, 2018, **370**, 129–223; (*c*) F. Bonnet, M. Visseaux, D. Barbier-Baudry, A. Hafid, E. Vigier, and M. M. Kubicki, *Inorg. Chem.*, 2004, **43**, 3682–3690.

2 (*a*) J. D. Rinehart, M. Fang, W. J. Evans and J. R. Long, *J. Am. Chem. Soc.*, 2011, **133**, 14236–14239; (*b*) K. Kawasaki, R. Sugiyama, T. Tsuji, T. Iwasa, H. Tsunoyama, Y. Mizuhata,

N. Tokitoh and A. Nakajima, *Chem. Commun.*, 2017, **53**, 6557–6560; (*c*) A. F. R. Kilpatrick, and F. G. N. Cloke, *Dalton. Trans*. 2017, **46**, 5587–5597; (*d*) A. F. R. Kilpatrick, F.-S. Guo, B. M. Day, A. Mansikkamäki, R. A. Layfield and F. G. N. Cloke, *Chem. Commun.*, 2018, **54**, 7085–7088; (e) J. D. Hilgar, M. G. Bernbeck and J. D. Rinehart, *J. Am. Chem. Soc*., 2019, **141**, 1913–1917.

3 F. T. Edelmann, *New J. Chem.*, 1995, **19**, 535–550.

4 R. G. Hayes and J. L. Thomas, *J. Am. Chem. Soc.*, 1969, **91**, 6876.

5 K. O. Hodgson and K. N. Raymond, *Inorg. Chem.*, 1972, **11**, 3030–3035.

6 (*a*) F. Mares, K. Hodgson and A. Streitwieser, Jr., *J. Organomet. Chem.*, 1970, **24**, C68–C70; (*b*) K. R. Meihaus and J. R. Long, *J. Am. Chem. Soc.*, 2013, **135**, 17952–17957; (*c*) T. G. Wetzel, S. Dehnen and P. W. Roesky, *Organometallics*, 1999, **18**, 3835–3842; (*d*) S. Anfang, G. Seybert, K. Harms, G. Geiseler, W. Massa and K. Z. Dehnicke, *Z. Anorg. Allg. Chem.*, 1998, **624**, 1187–1192; (*e*) S. A. Kinsley, A. Streitwieser, Jr. and A. Zalkin, *Organometallics*, 1985, **4**, 52–57; (*f*) G. W. Rabe, M. Zheng-Presse, J. A. Golen and A. L. Rheingold, *Acta. Cryst.*, 2003, **E59**, m255–m256; (*g*) T. R. Boussie, D. C. Eisenberg, J. Rigsbee, A. Streitwieser and A. Zalkin, *Organometallics*, 1991, **10**, 1922–1928; (*h*) U. Kilimann, M. Schäfer, R. Herbst-Irmer and F. T. Edelmann, *J. Organomet. Chem.*, 1994, **469**, C10–C14; (*i*) L. Ungur, J. J. Le Roy, I. Korobkov, M. Murugesu and L. F. Chibotaru, *Angew. Chem. Int. Ed.*, 2014, **53**, 4413–4417; (*j*) K. L. M. Harrimann, J. L. Brosmer, L. Ungur, P. L. Diaconescu and M. Murugesu, *J. Am. Chem. Soc.*, 2017, **139**, 1420–1423; (*k*) C. Meermann, K. Ohno, K. W. Törnroos, K. Mashima and R. Andwander, *Eur. J. Inorg. Chem.*, 2009, 76–85; (*l*) C. T. Palumbo, M. E. Fieser, J. W. Ziller and W. J. Evans, *Organometallics*, 2017, **36**, 3721–3728.

7 (*a*) J. Xia, Z. Jin and W. Chen, *J. Chem. Soc., Chem. Commun.*, 1991, **17**, 1214–1215; (*b*) J. J. Le Roy, L. Ungur, I. Korobkov, L. F. Chibotaru and M. Murugesu, *J. Am. Chem. Soc.*, 2004, **136**, 8003–8010.

8 T. Tsuji, N. Hosoya, S. Fukazawa, R. Sugiyama, T. Iwasa, H. Tsunoyama, H. Hamaki, N. Tokitoh and A. Nakajima, *J. Phys. Chem. C.*, 2014, **118**, 5896–5907.

9 C. W. DeKock, S. R. Ely, T. E. Hopkins and M. A. Brault, *Inorg. Chem.*, 1978, **17**, 625–631.

10 A. Streitwieser, Jr., U. Muller-Westerhoff, G. Sonnichsen, F. Mares, D. G. Morrell, K. O. Hodgson and C. A. Harmon, *J. Am. Chem. Soc.*, 1973, **95**, 8644–8649.

11 R. D. Shannon, *Acta Cryst.*, 1976, **A32**, 751–767.

12 (*a*) H. Schumann, J. Sun and A. Deitrich, *Monatsh. Chem.*, 1990, **121**, 747–753; (*b*) H. Schumann, J. Winterfeld, M. Glanz, R. D. Köhn and H. Hemling, *J. Organomet. Chem.*, 1994, **481**, 275–282; (*c*) P. W. Roesky, *J. Organomet. Chem.*, 2001, **621**, 277–283; (*d*) J. Gavenonis and T. D. Tilley, *J. Organomet. Chem.*, 2003, **689**, 870–878; (*e*) J. O. Moilanen, A. Mansikkamäki, M. Lahtinen, F. Guo, E. Kalenius, R. A. Layfield and L. F. Chibotaru, *Dalton Trans.*, 2017, **46**, 13582–13589; (*f*) W. J. Evans, J. C. Brady and J. W. Ziller, *J. Am. Chem. Soc.*, 2001, **123**, 7711–7712; (*g*) X. Li, J. Hong, R. Liu, L. Weng and X. Zhou, *Organometallics*, 2010, **29**, 4606–4610.

13 Q. Liu, X. Shen, J. Huang, Y. Qian, A. S. Chan and W. Wong, *Polyhedron*, 2000, **19**, 453–456.

14 N. V. Kozhemyakina, J. Nuss and M. Jansen, *Z. Anorg. Allg. Chem.*, 2009, **635**, 1355-1361.

15 Z. Zhou, J. Greenough, Z. Wei and M. A. Petrukhina, *Acta Cryst.,* 2017, **C73**, 420–423.

16 SAINT; part of Bruker APEX3 software package (version 2017.3-0): Bruker AXS, 2017.

17 SADABS; part of Bruker APEX3 software package (version 2017.3-0): Bruker AXS, 2017.2.

18 SHELXT; Version 2018/2: G. M. Sheldrick, *Acta Cryst.*, 2015, **A71**, 3–8.

19 XL refinement program version 2018/3: G. M. Sheldrick, *Acta Cryst.*, 2015, **C71**, 3-8.

Suggested TOC: